

Density-wave instability in a two-dimensional dipolar Fermi gas

Yasuhiro Yamaguchi

Research Center for Nuclear Physics, Osaka University, Ibaraki, Osaka 567-0047, Japan

Takaaki Sogo

Institut für Physik, Universität Rostock, D-18051 Rostock, Germany

Toru Ito

Department of Physics, Faculty of Science, Tokyo University of Science, 1-3 Kagurazaka, Shinjuku, Tokyo 162-8601, Japan

Takahiko Miyakawa*

Faculty of Education, Aichi University of Education, Hirosawa 1, Igaya-cho, Kariya 448-8542, Japan

(Received 10 March 2010; published 29 July 2010)

We consider a uniform dipolar Fermi gas in two dimensions (2D) where the dipole moments of fermions are aligned by an orientable external field. We obtain the ground state of the gas in the Hartree-Fock approximation and investigate random-phase-approximation stability against density fluctuations of finite momentum. It is shown that the density-wave instability takes place in a broad region where the system is stable against collapse. We also find that the critical temperature can be a significant fraction of Fermi temperature for a realistic system of polar molecules.

DOI: [10.1103/PhysRevA.82.013643](https://doi.org/10.1103/PhysRevA.82.013643)

PACS number(s): 03.75.Ss, 05.30.Fk, 67.85.-d, 05.30.Rt

I. INTRODUCTION

The realization of ultracold molecules confers remarkable opportunities to study new states of quantum matter and is also of much interest for quantum computing [1]. In particular, the investigation of polar molecules is a good candidate for studying various quantum many-body states because the anisotropic and long-range nature of the dipole-dipole interaction offers rich properties that do not occur in nondipolar systems [2].

Recently K.-K. Ni *et al.* succeeded in creating a dense gas of ^{40}K - ^{87}Rb polar molecules with temperature $T \approx 2.5T_F$ [3], where T_F is the Fermi temperature. For the absolute rovibrational ground state of the fermionic molecule attained in the experiment, the magnitude of the electric dipole moment is 0.566 D, yielding to significant interaction effects in a degenerate gas of dipolar fermions at lower temperatures. As shown in Ref. [4], the anisotropy of the dipole-dipole interaction results in a deformed Fermi surface of the ground state of a dipolar Fermi gas. Since the Fermi surface is the determining factor in low-energy properties of the Fermi system, theoretical studies of collective oscillations [5,6], stability [7], expansion dynamics after turning off the trapping potential [5,8], zero sound propagation in a homogeneous system [9,10], and equilibrium properties at finite temperatures [11–13] under the deformed Fermi surface have been done recently.

Some of most fascinating challenges of a dipolar Fermi gas concern phase transitions of possible ordered phases. So far, the realization of superfluid phase in three dimensions (3D) [14,15] and two dimensions (2D) [16,17], biaxial nematic phase [18], and ferromagnetic phase of two-component mixtures [19] have been proposed theoretically. Moreover, there is another interesting ordered phase arising from the repulsive part of the long-range dipole-dipole force, a density wave phase.

In a density wave phase, translational invariance is broken spontaneously, resulting in a distorted density distribution [20]. The phase transition of the charge density wave in a one-dimensional (1D) conductor was originally discussed by Peierls [21], who found the instability of a metallic state at zero temperature. In the mid-1970s, the charge and spin density waves were discovered in experiments and a number of interesting phenomena were found in static and dynamic properties of the density waves [22].

In the present article, we consider a uniform dipolar Fermi gas in 2D with the dipole moments aligned to an orientable external field. We study a realization of the phase transition of a density wave by evaluating the stability condition for the thermal equilibrium state in a random phase approximation (RPA). By calculating the critical temperature T_c , we show that the density wave can be achieved at a significant fraction of T_F for a realistic system of polar molecules. Here we note that the density wave is brought purely by the interaction effect in contrast to the density waves in an optical lattice potential as discussed in Refs. [23,24].

This article is organized as follows. Section II presents the mean field model of the uniform gas of fermions interacting via dipole-dipole forces in 2D. Section III presents the ground-state properties at zero temperature and discusses RPA stability. We obtain a phase diagram at zero temperature as a variance of the magnitude of the interaction strength and the angle between the direction of the dipole moments and normal direction of the 2D plane. Section IV applies our model to dipolar Fermi gases at finite temperatures, which leads to the critical temperature of the density-wave phase transition. Section V is a summary.

II. DIPOLAR FERMION GAS IN 2D

We consider a gas of dipolar fermions of mass m and electric or magnetic dipole moment \mathbf{d} . The dipoles are confined by

*takamiya@aecc.aichi-edu.ac.jp

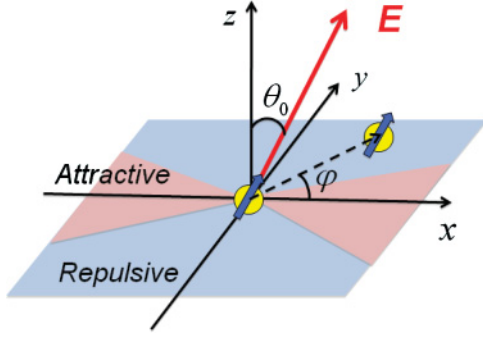


FIG. 1. (Color online) Experimental setup of 2D dipolar fermions. The dipole moments are aligned by an orientable external field, \mathbf{E} , that forms the angle θ_0 with respect to the z axis. The symbol φ denotes the azimuthal angle with respect to the x axis of the relative coordinate of two particles in the x - y plane.

a harmonic trapping potential $V(z) = m\omega_z^2 z^2/2$ with a trap frequency ω_z in the z direction. For $\hbar\omega_z \gg \epsilon_F$ where ϵ_F is the Fermi energy, the system is effectively 2D. The dipole moments are aligned by an external electric or magnetic field, \mathbf{E} , subtending an angle θ_0 with respect to the z axis as shown in Fig. 1. In this case, the Hamiltonian of the system is given by

$$\hat{H} = \sum_{i=1}^N -\frac{\hbar^2}{2m} \nabla_i^2 + \frac{1}{2} \sum_{i \neq j} V_{dd}(\mathbf{r}_i - \mathbf{r}_j), \quad (1)$$

where N is the number of fermions and \mathbf{r}_i is the position vector of i th particle in the x - y plane. The 2D dipole-dipole interaction in Eq. (1) is described by

$$\begin{aligned} V_{dd}(\mathbf{r}) &= \frac{d^2}{r^3} \{1 - 3 \sin^2 \theta_0 \cos^2 \varphi\} \\ &= \frac{d^2}{r^3} \left\{ P_2(\cos \theta_0) - \frac{3}{2} \sin^2 \theta_0 \cos 2\varphi \right\}, \end{aligned} \quad (2)$$

where φ is the azimuthal angle relative to the x axis; see Fig. 1. In this expression, we have a second-order Legendre polynomial, $P_2(\cos \theta_0) = (3 \cos^2 \theta_0 - 1)/2$. According to the procedure introduced in Ref. [10], the momentum representation of the 2D dipole-dipole interaction of Eq. (2) is given by $V_{dd}(\mathbf{q}) = V_0 + V_{2d}(\mathbf{q})$ where

$$V_0 = 2\pi d^2 P_2(\cos \theta_0) \frac{1}{r_c}, \quad (3)$$

$$V_{2d}(\mathbf{q}) = \pi d^2 q \{-2P_2(\cos \theta_0) + \sin^2 \theta_0 \cos 2\varphi\}. \quad (4)$$

In Eq. (4), φ is the angle with respect to the q_x axis. In Eq. (3), r_c is a cutoff length and an order of size of a dipolar particle, say, the size of a polar molecule, where the dipole moment is no longer an ideal dipole moment. Thus, the divergence in the limit of $r_c \rightarrow 0$ is artificial [25]. As we see, however, the total energy for dipolar fermions is always finite even in the limit of $r_c \rightarrow 0$. Thus, we do not need to pay attention to such an artificial divergence. Different treatment for the quasi-2D dipole-dipole interaction has been also discussed in Ref. [26].

The thermal equilibrium state of dipolar fermions at a temperature T is assumed to be translational invariant in the x - y plane. In the Hartree-Fock (HF) approximation, the total

energy per area derived from the Hamiltonian of Eq. (1) is represented by

$$E_{\text{tot}} = E_{\text{kin}} + E_{\text{int}}, \quad (5)$$

$$E_{\text{kin}} = \int \frac{d^2k}{(2\pi)^2} \frac{\hbar^2 \mathbf{k}^2}{2m} f(\mathbf{k}), \quad (6)$$

$$E_{\text{int}} = -\frac{1}{2} \int \frac{d^2k}{(2\pi)^2} \int \frac{d^2k'}{(2\pi)^2} f(\mathbf{k}) f(\mathbf{k}') V_{2d}(\mathbf{k} - \mathbf{k}'), \quad (7)$$

where $f(\mathbf{k})$ is the Fermi distribution function at T

$$f(\mathbf{k}) = \frac{1}{\exp\{[(\epsilon(\mathbf{k}) - \mu)/k_B T] + 1\}}, \quad (8)$$

with Boltzman constant k_B and the chemical potential μ . The single particle energy $\epsilon(\mathbf{k})$ is obtained by solving the self-consistent HF equation,

$$\epsilon(\mathbf{k}) = \frac{\hbar^2 \mathbf{k}^2}{2m} - \int \frac{d^2k'}{(2\pi)^2} V_{2d}(\mathbf{k} - \mathbf{k}') f(\mathbf{k}'), \quad (9)$$

under the constraint for the number density of fermions in 2D:

$$n_{2d} = \int \frac{d^2k}{(2\pi)^2} f(\mathbf{k}). \quad (10)$$

We note that the mean field interaction energy E_{int} of Eq. (7) is the sum of the direct and exchange energy, where a total cancellation of the short-range interaction V_0 of Eq. (3) occurs due to Fermi statistics. Thus, the divergence of V_0 in the limit of $r_c \rightarrow 0$ disappears in E_{int} or E_{tot} .

III. GROUND STATE AND STABILITY AT ZERO TEMPERATURE

In this section, we obtain the ground state at zero temperature $T = 0$ in the HF approximation where the distribution function is replaced by

$$f(\mathbf{k}) = \Theta(\epsilon_F - \epsilon(\mathbf{k})), \quad (11)$$

with $\mu = \epsilon_F$. In this equation, $\Theta()$ denotes Heaviside's step function. When the external field tilts with respect to the z axis, the anisotropy of $V_{2d}(\mathbf{q})$ in the 2D momentum space causes the deformed Fermi surface. Before the study of numerical calculations in the HF approximation, we introduce a variational approach that captures physical insight of the ground state.

A. Variational method

In Refs. [4,5], we developed a variational method (VM) to a 3D dipolar Fermi gas, which describes the deformed Fermi surface with an ellipsoidal shape. In Ref. [16], Bruun and Taylor applied the VM to a 2D dipolar Fermi gas with the variational density distribution

$$f(\mathbf{k}) = \Theta \left(k_{F0}^2 - \alpha^2 k_x^2 - \frac{1}{\alpha^2} k_y^2 \right), \quad (12)$$

where the positive parameter α describes an elliptical Fermi surface and $k_{F0} \equiv \sqrt{4\pi n_{2d}}$. When $\theta_0 \neq 0$, the minus sign of the interaction energy (7) and the anisotropy of $V_{2d}(\mathbf{q})$ tend to stretch the Fermi surface along the x axis, leading to $\alpha < 1$.

Under the assumption of the distribution function of Eq. (12), the total energy in VM in units of $\hbar^2 n_{2d}^2/m$ is given by (see Appendix)

$$\mathcal{E}_{\text{tot}} = \frac{\pi}{2} \left(\frac{1}{\alpha^2} + \alpha^2 \right) - \frac{32}{15} g I(\alpha; \theta_0), \quad (13)$$

where $g \equiv 4md^2 k_{F0}/3\pi\hbar^2$ and $I(\alpha; \theta_0)$ is defined by

$$I(\alpha; \theta_0) \equiv -\frac{2P_2(\cos \theta_0)}{\alpha} E(1-\alpha^4) + \frac{\sin^2 \theta_0}{\alpha} \left\{ -\frac{2\alpha^4}{1-\alpha^4} K(1-\alpha^4) + \frac{1+\alpha^4}{1-\alpha^4} E(1-\alpha^4) \right\} \quad (14)$$

for $\alpha < 1$ and $I(\alpha; \theta_0) = -\pi$ for $\alpha = 1$. In Eq. (14), $K(m)$ and $E(m)$ are the complete elliptic integrals of the first and second kind defined by

$$K(m) = \int_0^{\pi/2} d\theta \frac{1}{\sqrt{1-m\sin^2\theta}}, \quad (15)$$

$$E(m) = \int_0^{\pi/2} d\theta \sqrt{1-m\sin^2\theta}, \quad (16)$$

respectively. We find the VM ground state by minimizing the total energy (13), giving rise to an optimized variational parameter $\alpha = \alpha_0$.

B. Ground-state properties

Figure 2 shows the deformed Fermi surface in the 2D momentum space in units of k_{F0} for $g = 1.0$ and $\theta_0 = \arccos(1/\sqrt{3})$ where $P_2(\cos \theta_0) = 0$. The crosses and solid line correspond to results from numerical calculations in the HF approximation and VM, respectively. It is shown that the two results match very well, as is the case for a 3D dipolar Fermi gas [9], and the Fermi wave number derived from $\epsilon_F = \epsilon(\mathbf{k})$, $k_F(\phi)$, is dependent on ϕ . In Fig. 3, we plot the aspect ratio of the Fermi surface, $k_F(\pi/2)/k_F(0)$, of the HF and VM ground state as a function of g for $\theta_0 = 0.1\pi, 0.2\pi, \arccos(1/\sqrt{3})$. We note that the aspect ratio in VM is given by $k_F(\pi/2)/k_F(0) = \alpha_0^2$; see Eq. (12). This result reveals that the shape of Fermi surface is well approximated by the elliptical shape for different values of g and θ_0 .

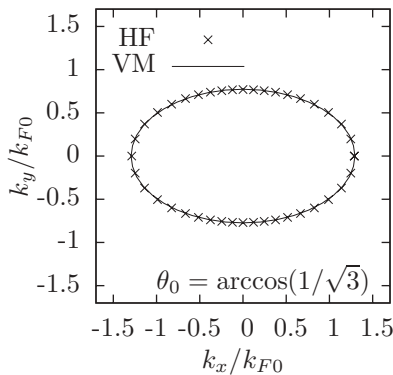


FIG. 2. Deformed Fermi surface for $g = 1.0$ and $\theta_0 = \arccos(1/\sqrt{3})$ derived from numerical calculations in the HF approximation (crosses) and VM (solid line).

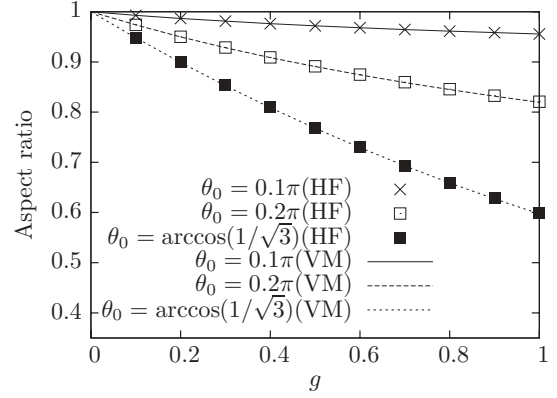


FIG. 3. Aspect ratio of the Fermi surface, $k_F(\pi/2)/k_F(0)$, as a function of g for $\theta_0 = 0.1\pi, \theta_0 = 0.2\pi$, and $\theta_0 = \arccos(1/\sqrt{3})$ from top to bottom. The crosses, blank squares, and filled squares are results of the HF ground state, and the solid line, dashed line, and dotted line are results of the VM ground state.

We numerically calculate the Fermi energy, ϵ_F , by a partial derivative of the total energy of the system with respect to the number density n_{2d} . Figure 4 shows a plot of ϵ_F in units of $\hbar^2 n_{2d}/m$ of the HF and VM ground state as a function of g for different values of θ_0 . Again, two of the results agree very well. As g increases, ϵ_F increases for $\theta_0 = 0.1\pi, 0.2\pi$ and decreases for $\theta_0 = \arccos(1/\sqrt{3})$. This result reveals that an average effect of $V_{2d}(\mathbf{q})$ turns from repulsive to attractive as the direction of the external field is further apart from the z axis.

C. Stability condition

We examine the stability of the ground state and obtain a phase diagram at zero temperature in the g - θ_0 plane. To judge the stability of the system, we take the RPA [27,28] and obtain the stability condition

$$1 + V_{2d}(\mathbf{q})\chi(\mathbf{q}) > 0, \quad (17)$$

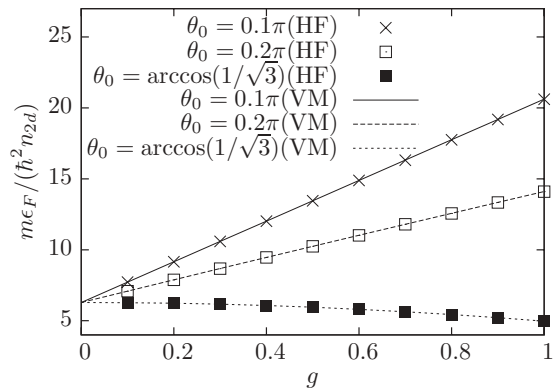


FIG. 4. Fermi energy as a function of g for $\theta_0 = 0.1\pi, \theta_0 = 0.2\pi$, and $\theta_0 = \arccos(1/\sqrt{3})$ from top to bottom. The crosses, blank squares, and filled squares are results of the HF ground state, and the solid line, dashed line, and dotted line are results of the VM ground state.

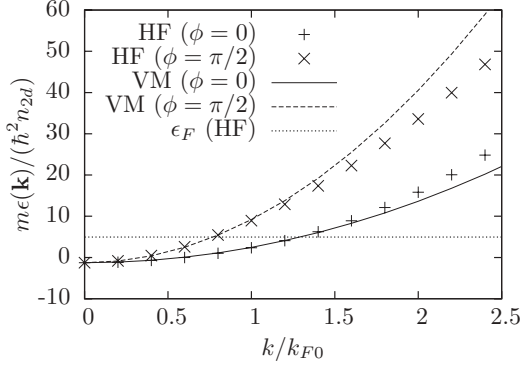


FIG. 5. Single-particle energies $\epsilon(k, \phi = 0)$ and $\epsilon(k, \phi = \pi/2)$ for $g = 1.0$ and for $\theta_0 = \arccos(1/\sqrt{3})$ derived from numerical calculations in the HF approximation (crosses and pluses) and VM (solid and dashed lines). The dotted line represents the Fermi energy in the HF approximation.

where $\chi(\mathbf{q})$ is the density-density response function against density fluctuations of finite momentum \mathbf{q} defined by

$$\chi(\mathbf{q}) = \int \frac{d^2k}{(2\pi)^2} \frac{f(\mathbf{k} + \mathbf{q}) - f(\mathbf{k})}{\epsilon(\mathbf{k}) - \epsilon(\mathbf{k} + \mathbf{q})}. \quad (18)$$

As we have seen in the previous subsection, the aspect ratio and the Fermi energy in VM approximate to those in the HF approximation quite well. Thus, we calculate the response function by use of the single-particle energy that reproduces the variational distribution function (12). The single-particle energy in VM reads

$$\epsilon(\mathbf{k}) = \epsilon(\mathbf{0}) + \frac{\hbar^2}{2m} \lambda^2 \left(\alpha_0^2 k_x^2 + \frac{1}{\alpha_0^2} k_y^2 \right), \quad (19)$$

$$\epsilon(\mathbf{0}) = -\frac{\hbar^2 k_{F0}^2}{4m} g I(\alpha_0, \theta_0), \quad (20)$$

where λ represents the curvature of the single-particle energy and is determined by the relationship

$$\epsilon_F = \epsilon(\mathbf{0}) + \lambda^2 \frac{\hbar^2 k_{F0}^2}{2m}. \quad (21)$$

Figure 5 shows the single-particle energy in the HF approximation and VM as a function of $k = |\mathbf{k}|$ at $\phi = 0$ and $\pi/2$. The single-particle energy in the VM matches with that in the HF approximation below and near the Fermi energy. This result reveals that the ground-state properties such as Fermi surface (Fig. 2), aspect ratio (Fig. 3), and Fermi energy (Fig. 4) are properly reproduced by the VM.

By use of the density distribution (12) and single-particle energy (19) in Eq. (18), the analytic form of the response function for $\mathbf{q} = (q, \phi)$ is obtained by

$$\chi(\mathbf{q}) = \frac{m}{2\pi \lambda^2 \hbar^2} \left[1 - \sqrt{1 - \left(\frac{2k_F(\phi)}{q} \right)^2} \Theta(q - 2k_F(\phi)) \right], \quad (22)$$

where the angle-dependent Fermi wave number is given by

$$k_F(\phi) = \frac{k_{F0}}{\sqrt{\alpha_0^2 \cos^2 \phi + \frac{1}{\alpha_0^2} \sin^2 \phi}}. \quad (23)$$

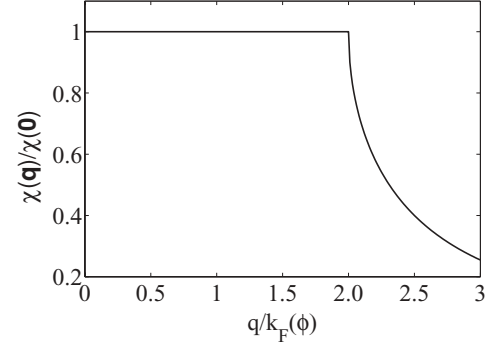


FIG. 6. Density-density response function in VM.

We plot $\chi(\mathbf{q})$ of Eq. (22) in Fig. 6 that is constant below $q \leq 2k_F(\phi)$, monotonically decreasing for $q > 2k_F(\phi)$, and shows a singular behavior at $q = 2k_F(\phi)$.

Apart from $\theta_0 = 0$, the 2D dipolar interaction $V_{2d}(\mathbf{q})$ is anisotropic and is most negative at $\phi = \pi/2$ for a fixed magnitude of momentum q . Thus the system is expected to be unstable against density fluctuations of the momentum $\mathbf{q} = (q, \pi/2)$. Once the condition

$$V_{2d}\left(q, \frac{\pi}{2}\right) \chi\left(q, \frac{\pi}{2}\right) \leq -1 \quad (24)$$

is fulfilled, the system becomes unstable. The minimum value of the left-hand side of Eq. (24) occurs at $q = 2k_F(\pi/2) = 2\alpha_0 k_{F0}$. Thus, we obtain the instability condition of the system as

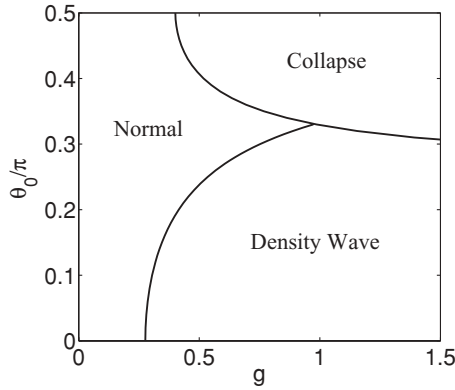
$$g \cos^2 \theta_0 \frac{\alpha_0}{\lambda^2} \geq \frac{2}{3\pi} = 0.212. \quad (25)$$

In case this condition is satisfied, the density fluctuation of the momentum $q = 2\alpha_0 k_F$ along the y axis starts to develop. This indicates that the phase transition from a normal-phase gas into a density-wave phase takes place for larger g and smaller θ_0 . Note that the expected density wave is a planar wave transverse to the dipolar direction. As shown in the instability condition (25), the system becomes unstable even when $\theta_0 = 0$ that corresponds to the circular symmetric system. In this case, the density wave of a spherical wave is possible to appear as a stable ground state.

In density-wave instability, there are two key ingredients, that is, the linear momentum dependence of $V_{2d}(\mathbf{q})$ and the singular behavior of $\chi(q, \pi/2)$ at $q = 2\alpha_0 k_{F0}$. Thus, the present mechanism of the density-wave instability in 2D dipolar Fermi gases arises from the combined effects of the long-range nature of the dipole-dipole interaction and the Fermi surface effect in the 2D system. For 3D dipolar Fermi gases, the dipole-dipole interaction does not depend on the magnitude of momentum [4], and the Fermi surface effect is less significant. Thus, the density-wave phase may not appear in the 3D system.

Figure 7 shows a phase diagram at zero temperature in terms of g and θ_0 . While the density-wave instability is identified by Eq. (25), the collapse instability is identified with a negative value of the inverse compressibility, $\kappa^{-1} < 0$ where

$$\kappa^{-1} = \frac{2\hbar^2 n_{2d}}{m} \left[\mathcal{E}_{\text{tot}} + \frac{7}{8} g \frac{\partial \mathcal{E}_{\text{tot}}}{\partial g} + \frac{1}{8} g^2 \frac{\partial^2 \mathcal{E}_{\text{tot}}}{\partial g^2} \right]. \quad (26)$$


 FIG. 7. Phase diagram at zero temperature in terms of g and θ_0 .

This result reveals that the density-wave phase transition takes place in a broad region for larger g and smaller θ_0 where the system is stable against collapse [29].

IV. CRITICAL TEMPERATURE OF THE DENSITY-WAVE PHASE TRANSITION

In this section, we apply our analysis for RPA stability into dipolar Fermi gases at finite temperatures and obtain the critical temperature of the density-wave phase transition.

To do so, we judge the stability condition (17) with the density-density response function (18) using the single-particle energy calculated by the self-consistent HF equation (9) at a finite T without the variational ansatz. A critical temperature of the phase transition, T_c , is the highest temperature at which the condition

$$V_{2d}\left(q, \frac{\pi}{2}\right)\chi\left(q, \frac{\pi}{2}; T_c\right) = -1 \quad (27)$$

is fulfilled.

Figure 8 shows T_c in units of ideal gas Fermi temperature $T_F^0 \equiv \hbar^2 k_{F0}^2 / 2mk_B$, as a function of g for $\theta_0 = 0$ (crosses), $\theta_0 = 0.2\pi$ (asterisks), and $\theta_0 = \arccos(1/\sqrt{3})$ (squares). In Fig. 8, we also plot results by replacing $\epsilon(\mathbf{k})$ in Eq. (8) with the VM single-particle energy of Eq. (19) where λ and α_0

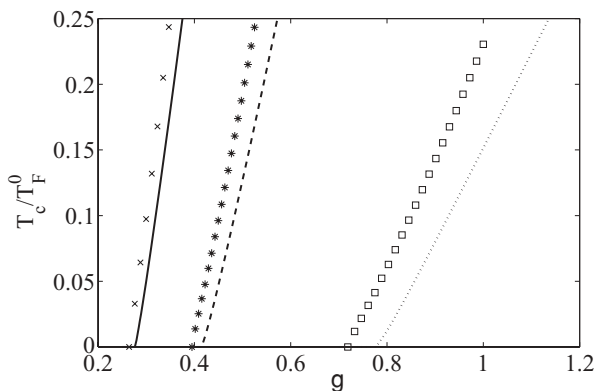


FIG. 8. Critical temperature T_c with the HF single-particle energy as a function of g for $\theta_0 = 0$ (crosses), $\theta_0 = 0.2\pi$ (asterisks), and $\theta_0 = \arccos(1/\sqrt{3})$ (squares). The solid line, dashed line, and dotted line are T_c with the VM single-particle energy for $\theta_0 = 0, 0.2\pi$, and $\arccos(1/\sqrt{3})$, respectively.

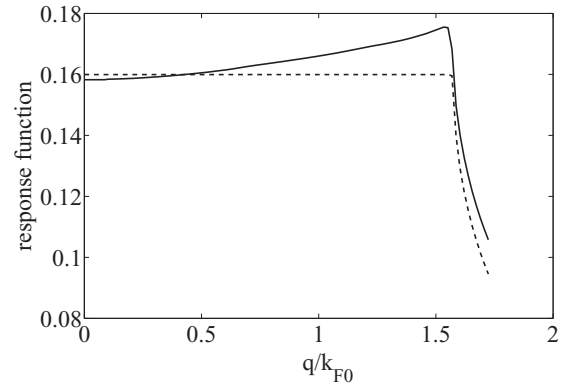


FIG. 9. Density-density response function in units of m/\hbar^2 for $g = 0.928$, $\theta_0 = \arccos(1/\sqrt{3})$, and $T = 0.02T_F^0$ in the HF approximation (solid line) and VM (dashed line).

are results of the corresponding system at zero temperature. The critical temperature with the HF single-particle energy is higher than that with the VM single-particle energy for same g and θ_0 . This indicates that the response function $\chi(q, \pi/2)$ at around $q = k_F(\pi/2)$ in the HF approximation is larger than that in the VM as shown in Fig. 9. This is a consequence of overestimates at $k > k_F(\pi/2)$ for the VM single-particle energy, as shown in Fig. 5, which leads to a decrease of the response function via the denominator of the integrand in Eq. (18).

It is well known that the charge density-wave instability in the 1D conductor is due to the nesting property, that is, the increase of the number of lower energy excitations of particle-hole pairs near the Fermi surface [22]. The fact that the curvature of the single-particle energy at $\phi = \pi/2$ in the HF approximation is lower than that in VM brings a large enhancement of the nesting property for a highly deformed Fermi surface. As shown in Fig. 8, the difference between the two results is remarkable for larger θ_0 . Thus, we conclude that the deformation of the Fermi surface furthers the density-wave phase transition.

Finally, let us consider how high the critical temperature will be for a realistic system. For ^{40}K - ^{87}Rb polar molecules with the electric dipole moment of 0.566 D observed by JILA group [3], $m = 127$ u, and with the number density of $2.0 \times 10^7 \text{ cm}^{-2}$, we have $g = 0.409$. Figure 10 reveals that T_c increases with decreasing θ_0 and can be a significant fraction of T_F . Such a high critical temperature suggests that the density

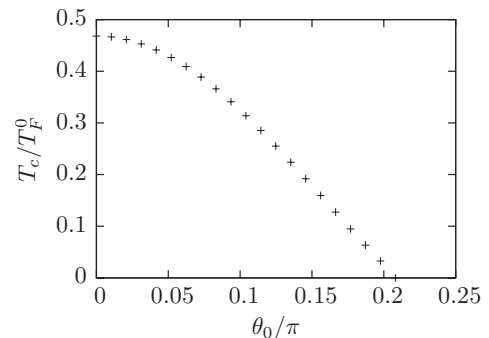


FIG. 10. Critical temperature T_c as a function of θ_0 for $g = 0.409$.

wave of fermionic polar molecules can be observed in future experiments [30].

V. SUMMARY

In the present article, we have studied a realization of the density-wave phase transition in a 2D dipolar Fermi gas where the dipole moments of fermions are aligned by an orientable external field. To judge the stability of a normal gas, we have investigated RPA stability against density fluctuations of finite momentum. We showed that the density-wave instability takes place in a broad region where the system is stable against collapse. We found that the critical temperature T_c of the phase transition in the mean field approximation can be achieved at a significant fraction of T_F for a realistic system of polar molecules.

As discussed in Ref. [16], the superfluid phase transition of p -wave Cooper pairs is possible to realize for $\theta_0 \gtrsim \arcsin(2/3) = 0.23\pi$ at $T = 0$. The combination of this and our conclusions offers a challenging quest for a coexisting phase of the superfluid and density-wave orders in a 2D dipolar Fermi gas. This will be discussed in a future publication.

Note added. Recently, we found a preprint by Sun, Wu, and Das Sarma [31] where the density-wave instability in a 2D dipolar Fermi gas at zero temperature was studied with results agree with those presented here.

ACKNOWLEDGMENTS

We are very grateful to Dr. A. Suzuki for his continuous encouragement and useful discussions at Tokyo University of Science, where much of the work was done. TM acknowledges helpful discussions with Dr. H. Pu and his hospitality at Rice University, where part of the work was completed. TM also thanks Dr. T. Nikuni for useful comments. TS is supported by the DFG Grant No. RO905/29-1.

APPENDIX: CALCULATION OF VARIATIONAL ENERGY

In this appendix, we obtain the variational energy at zero temperature under the assumption of the variational distribution function (12). The total energy in the HF approximation is composed of the kinetic energy E_{kin} and interaction energy E_{int} defined by Eqs. (6) and (7), respectively.

First, the kinetic energy is easily obtained by

$$E_{\text{kin}} = \frac{\hbar^2 n_{2d}^2 \pi}{2m} \left(\frac{1}{\alpha^2} + \alpha^2 \right). \quad (\text{A1})$$

Next, we calculate the interaction energy

$$\begin{aligned} E_{\text{int}} &= -\frac{1}{2} \int \frac{d^2 k}{(2\pi)^2} \int \frac{d^2 k'}{(2\pi)^2} f(\mathbf{k}) f(\mathbf{k}') V_{2d}(\mathbf{k} - \mathbf{k}') \\ &= -\frac{4d^2}{\pi^3} k_{F0}^5 I(\alpha; \theta_0) C, \end{aligned}$$

where $I(\alpha; \theta_0)$ is defined by Eq. (14) and

$$C = \int_0^\infty dx x^2 \int_0^\infty dy y \int_0^{\pi/2} d\phi \Theta(1 - x^2 - y^2 - 2xy \cos \phi).$$

We define the function $f(\phi)$ as

$$f(\phi) = 1 - x^2 - y^2 - 2xy \cos \phi \geq f_{\min},$$

where $f_{\min} = 1 - (x + y)^2$. If $f_{\min} \geq 0$, then $\Theta(f(\phi)) = 1$ for $0 \leq \phi \leq \pi/2$; otherwise, $\Theta(f(\phi)) = 1$ for $\phi_0 \leq \phi \leq \pi/2$ and $\Theta(f(\phi)) = 0$ for $0 \leq \phi < \phi_0$ where the angle ϕ_0 is determined by $f(\phi_0) = 0$, that is

$$\phi_0 = \arccos \left(\frac{1 - x^2 - y^2}{2xy} \right).$$

With $C = C_1 - C_2$, where

$$C_1 = \frac{\pi}{2} \int_0^1 dx x^2 \int_0^{\sqrt{1-x^2}} dy y = \pi/30$$

and

$$\begin{aligned} C_2 &= \int_0^1 dx x^2 \int_{1-x}^{\sqrt{1-x^2}} dy y \arccos \left(\frac{1 - x^2 - y^2}{2xy} \right) \\ &= \pi/30 - 2/45, \end{aligned}$$

we obtain the interaction energy as

$$E_{\text{int}} = -\frac{32 \hbar^2 n_{2d}^2}{15 m} g I(\alpha; \theta_0). \quad (\text{A2})$$

Combining Eq. (A1) and Eq. (A2), we obtain the variational energy as

$$E_{\text{tot}} = \frac{\hbar^2 n_{2d}^2}{m} \left[\frac{\pi}{2} \left(\frac{1}{\alpha^2} + \alpha^2 \right) - \frac{32}{15} g I(\alpha; \theta_0) \right]. \quad (\text{A3})$$

-
- [1] L. D. Carr, D. Demille, R. V. Krems, and J. Ye, *New J. Phys.* **11**, 055049 (2009).
[2] M. A. Baranov, *Phys. Rep.* **464**, 71 (2008).
[3] K.-K. Ni, S. Ospelkaus, M. H. G. de Miranda, A. Pe'er, B. Neyenhuis, J. J. Zirbel, S. Kotochigova, P. S. Julienne, D. S. Jin, and J. Ye, *Science* **322**, 231 (2008).
[4] T. Miyakawa, T. Sogo, and H. Pu, *Phys. Rev. A* **77**, 061603(R) (2008).
[5] T. Sogo, L. He, T. Miyakawa, S. Yi, H. Lu, and H. Pu, *New J. Phys.* **11**, 055017 (2009).
[6] M. Tohyama, *J. Phys. Soc. Jpn.* **78**, 104003 (2009).
[7] J.-N. Zhang and S. Yi, *Phys. Rev. A* **80**, 053614 (2009).
[8] T. Nishimura and T. Maruyama, *J. Phys. Soc. Jpn.* **79**, 083001 (2010).
[9] S. Ronen and J. Bohn, *Phys. Rev. A* **81**, 033601 (2010).
[10] C.-K. Chan, C. Wu, W.-C. Lee, and S. Das Sarma, *Phys. Rev. A* **81**, 023602 (2010).
[11] J.-N. Zhang and S. Yi, *Phys. Rev. A* **81**, 033617 (2010).
[12] J. P. Kestner and S. Das Sarma, e-print arXiv:1001.4763.
[13] Y. Endo, T. Miyakawa, and T. Nikuni, *Phys. Rev. A* **81**, 063624 (2010).
[14] M. A. Baranov, M. S. Mar'enko, V. S. Rychkov, and G. V. Shlyapnikov, *Phys. Rev. A* **66**, 013606 (2002); M. A. Baranov, L. Dobrek, and M. Lewenstein, *Phys. Rev. Lett.* **92**, 250403 (2004).

- [15] C. Zhao, L. Jiang, X. Liu, W. M. Liu, X. Zou, and H. Pu, *Phys. Rev. A* **81**, 063642 (2010).
- [16] G. M. Bruun and E. Taylor, *Phys. Rev. Lett.* **101**, 245301 (2008).
- [17] N. R. Cooper and G. V. Shlyapnikov, *Phys. Rev. Lett.* **103**, 155302 (2009).
- [18] B. M. Fregoso, K. Sun, E. Fradkin, and B. L. Lev, *New J. Phys.* **11**, 103003 (2009).
- [19] B. M. Fregoso and E. Fradkin, *Phys. Rev. Lett.* **103**, 205301 (2009).
- [20] H. Fröhlich, *Proc. R. Soc. London A* **223**, 296 (1954).
- [21] R. E. Peierls, *Quantum Theory of Solids* (Oxford University Press, New York, 1955).
- [22] G. Grüner, *Density Waves in Solids* (Addison-Wesley Longman, Reading, MA, 1994).
- [23] J. Quintanilla, S. T. Carr, and J. J. Betouras, *Phys. Rev. A* **79**, 031601(R) (2009).
- [24] C. Lin, E. Zhao, and W. V. Liu, *Phys. Rev. B* **81**, 045115 (2010).
- [25] For dipolar fermions trapped in a tight harmonic potential $V(z)$, the wave function along the z axis is the Gaussian function with the width $d_z = \sqrt{\hbar/m\omega_z}$. In this case, the effective 2D dipole-dipole interaction is obtained by integrating out z degree of freedom. The resulting interaction has no divergence and shows the same linear momentum dependence as $V_{2d}(\mathbf{q})$ under the condition $k_{F0}d_z \ll 1$, which has to be fulfilled for effectively 2D Fermi systems. See Ref. [26].
- [26] U. R. Fischer, *Phys. Rev. A* **73**, 031602(R) (2006).
- [27] P. Nozieres and D. Pines, *The Theory of Quantum Liquid* (Perseus, Cambridge, 1999).
- [28] In RPA, we neglect the exchange scattering in particle-hole excitations; see Ref. [27]. For the stability condition against density fluctuations of finite momentum $\mathbf{q} = 2k_{F0}\hat{y}$, the direct scattering of particle-hole excitations dominates over the exchange one because of the linear momentum dependence of $V_{2d}(\mathbf{q})$.
- [29] This conclusion holds in the HF approximation. The discrepancy between results obtained by the two methods is only quantitative and is less than 10% as shown in the critical value of g at $T = 0$ in Fig. 8.
- [30] The density-wave phase transition in the 2D system that belongs to the Kosterlitz-Thouless universality class beyond the mean field approximation is briefly discussed in Ref. [31]. The mean field critical temperature presented here nevertheless offers useful information on the phase transition in the system and also in a system of an array of 2D dipolar Fermi gases tightly confined by a 1D optical lattice potential where the long-range order of the density wave is possible to remain at finite temperatures.
- [31] K. Sun, C. Wu, and S. Das Sarma, e-print [arXiv:1003.2757](https://arxiv.org/abs/1003.2757).